Inhalation Toxicology, 2009; 21(S1): 83–91

informa
healthcare

RESEARCH ARTICLE

Subacute intratracheal exposure of rats to manganese nanoparticles: Behavioral, electrophysiological, and general toxicological effects

Leila Sárközi[1], Endre Horváth[2], Zoltán Kónya[2], Imre Kiricsi[2], Brigitta Szalay[3], Tünde Vezér[1], and András Papp[1]

[1]Department of Public Health, University of Szeged Faculty of Medicine, Szeged, Hungary, [2]Department of Applied Chemistry, University of Szeged Faculty of Science, Szeged, Hungary, and [3]National Institute of Environmental health, Budapest, Hungary

Abstract

The toxicity of manganese-containing airborne particles is an important occupational and environmental problem. In this work, adult male Wistar rats were treated with a nanosuspension of MnO_2 of approximately 23 nm nominal particle diameter, instilled into the trachea for 3, 6, and 9 wk in doses of 2.63 and 5.26 mg Mn/kg. The animals' body weight was checked weekly. At the end of treatment, the rats' spontaneous motility was tested in an open field box. Then, spontaneous and stimulus-evoked cortical activity and action potential of the tail nerve were recorded in urethane anesthesia. The rats were finally dissected, organs weights were measured, and the presence of excess Mn in lung and brain samples was determined using scanning electron microscopy with energy-dispersive x-ray spectroscopy. While control rats had normal weight gain, the body weights of the treated rats ceased to grow from wk 6 on. The relative weight of the lungs increased in the treated rats, and that of the liver decreased, in a dose- and time-dependent manner; Mn was detected in their lung and brain samples. In the open field activity, the percentage of ambulation and rearing decreased while local activity and immobility increased. The latency of the evoked potentials was lengthened, and the conduction velocity of the tail nerve decreased. These results indicate that the Mn content of instilled nanoparticles had access from the airways to the brain, and the resulting damage could be investigated in animals using neuro-functional and general toxicological endpoints.

Keywords: *Behavior; body weight; electrophysiology; intratracheal instillation; manganese; nanoparticle; organ weight*

Introduction

Manganese (Mn) is an essential trace element, required for the development and normal working of the brain (Elder et al., 2006) but affecting its functions in excessive amounts. Within the organism, Mn has a tropism for tissues rich in mitochondria (liver, muscles, brain etc.) and is the activating constituent of metalloenzymes such as glutamine synthetase, superoxide dismutase (SOD), and pyruvate carboxylase (Erikson et al., 2003). In the central nervous system, glutamine synthetase catalyzes the conversion of glutamic acid to glutamine, thereby removing the transmitter. The enzyme requires Mn but is inhibited by its excess (Normandin and Hazell, 2002). Inhalational exposure to Mn in humans has been found to trigger Parkinson-like syndrome (Bowler et al., 2006; Kenangil et al., 2006), myoclonic movements (Ono et al., 2002), or epileptic syndrome (Hernandez et al., 2003). Increased latency of cortical evoked response, acoustic P-300, from exposed humans has also been reported (Wennberg et al., 1991).

The occupational environment in manganese ore processing, metallurgy, and metalworking is a major source of inhalational Mn exposure, as is the manufacturing of dry cell batteries (Bader et al., 1999) and application of organo-Mn fungicides (Ferraz et al., 1988). Inhalation of Mn-containing aerosol (dust, fume, mist) results—in miners, welders, smelters, etc.—in internal doses well above the usual environmental background (Roels et al., 1997). Methylcyclopentadienyl manganese tricarbonyl (MMT), added to unleaded gasoline

Address for Correspondence: András Papp, Department of Public Health, University of Szeged Faculty of Medicine, Dóm tér 10., H-6720 Szeged, Hungary. E-mail: ppp@puhe.szote.u-szeged.hu

(Received 01 April 2009; accepted 01 April 2009)

ISSN 0895-8378 print/ISSN 1091-7691 online © 2009 Informa UK Ltd
DOI: 10.1080/08958370902939406

as an antiknock agent in certain countries, leads to Mn emissions in the atmosphere, which may be a significant source of exposure to inorganic Mn in urban areas (Normandin et al., 2004). In case of inhalational exposure, Mn is likely to reach its target sites before hepatic clearance (by biliary excretion: Elder et al., 2006; Fechter et al., 2002), resulting in increased toxicity (Roels et al., 1997).

In cases of exposure by Mn-containing dusts and fumes, particle size is a most important factor. There are significant differences between nanoparticles (NPs) and larger particles regarding their behavior during deposition and clearance in the airways (Elder et al., 2006). Deposition of inhaled manganese NPs in the respiratory tract is mainly due to free diffusion driven by collision of the particles with air molecules (Oberdörster et al., 2005). Once deposited, systemic and central nervous system (CNS) exposure can result from transcytosis of the Mn-containing NPs (Oberdörster et al., 2005) or from dissolution of ionic Mn from their surface, first of all after ingestion by the macrophages (Lundborg et al., 1985).

In the present study, rats were treated by intratracheal instillation of manganese-containing nanoparticles (chemically, MnO_2) for 3 to 9 wk, as a model of inhalational exposure. The effects on body and organ weights and on electrophysiological and behavioral parameters were investigated.

Methods

Animals and treatment

Adult male Wistar rats (10 wk old, 320–350 g body weight) were obtained at the university's breeding centre and were housed in an air-conditioned room maintained at 22°C with a 12-h light/dark cycle (light on at 06:00), and free access to tap water and standard pelleted feed. The rats were divided into 4 groups of 24 animals each at the start (untreated control, vehicle control, low dose, high dose; see Table 1).

Nanostructured MnO_2 (mean diameter: 23.2 ± 3.3 nm) was synthesized at the Department of Applied Chemistry by a technique combining sonication and hydrothermal treatment. An appropriate amount of aqueous $KMnO_4$ solution was mixed with ethylene glycol and sonicated with Hielscher UIP1000 ultrasound device. The resulted dark suspension was loaded into a Teflon-lined stainless steel autoclave. The autoclave was heated at 200°C for 16 h in an oven and then allowed to cool to room temperature naturally. The brownish precipitate formed was filtered and washed with 80°C preheated water to remove any unreacted starting material and the soluble by-products formed during the reaction. The precipitate was dried at 100°C for 1 h. Its chemical purity was checked by x-ray diffraction, and its particle size, by x-ray diffraction and transmission electron microscopy. The particle size histogram and a transmission electron microscopy (TEM) picture are shown in Figure 1.

For administration to the rats, the nanosuspension was diluted in distilled water, and was instilled into each rat's trachea in doses corresponding to 2.63 (low dose, LD) or 5. 26 mg (high dose, HD) Mn/kg body weight, 5 days per week (Monday to Friday) for 3, 6, and 9 wk. That is, 8 rats from each groups were sacrificed after 3 wk of treatment, another 8 after 6 wk, etc. There was an untreated control (Con, neither ether anesthesia nor instillation) and a water control (W, anesthetized and instilled with distilled water) group. The treatment scheme of the experiment is shown in Table 1. For intratracheal instillation, the animals

Table 1. Treatment groups and the corresponding doses.

Group	Code	Treatment and dose	Duration
Untreated control	Con	—	
Vehicle control	W	Distilled water 1 ml/kg body weight	
Low dose	LD	MnO_2 nanosuspension, 2. 63 mg Mn/kg body weight; 1 ml/kg body weight	3, 6, and 9 wk in all groups*
High dose	HD	MnO_2 nanosuspension, 5. 26 mg Mn/kg body weight; 2 ml/kg body weight	

*The groups started with 24 rats each; 8 rats per group were processed and sacrificed after 3, 6, and 9 wk of treatment, respectively.

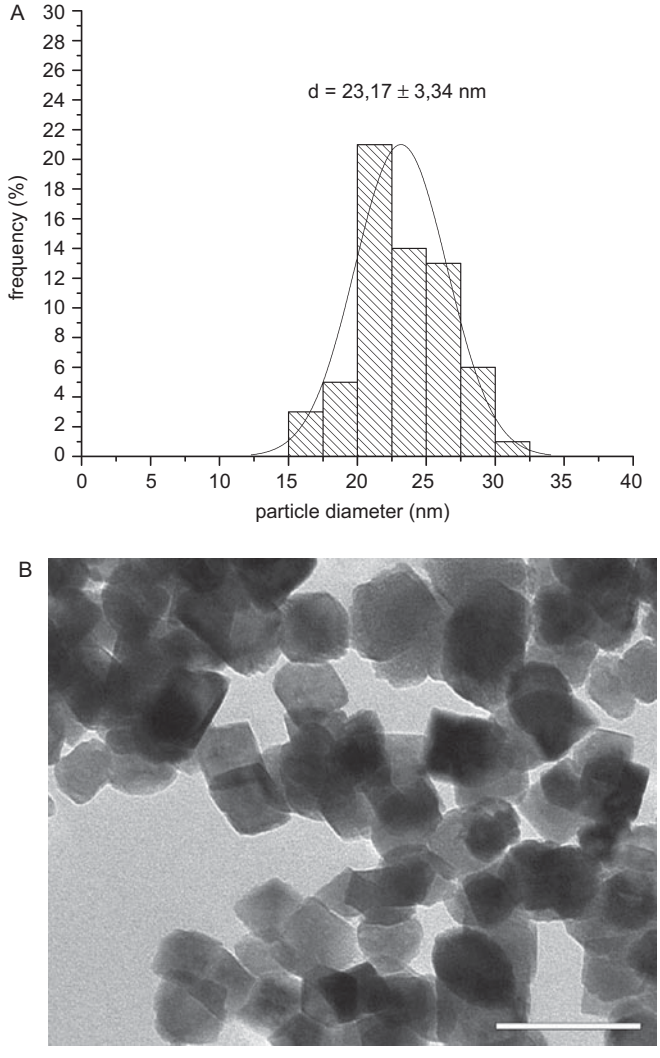

Figure 1. Size distribution histogram (A) and TEM picture (B) of the MnO_2 nanoparticles. The distribution was determined by x-ray diffraction. Scale bar for B: 50 nm.

were anesthetized with diethyl ether in a glass jar with an air-tight lid. As soon as the anesthesia was complete, the animal was suspended on an oblique board, standing at 60° to horizontal, with its upper incisors hung in a wire loop to hold the animal in place and keep its mouth open (Oka et al., 2006). The trachea was illuminated transdermally by means of a fiber optic light guide brought into direct contact with the animal's neck. The tongue was pulled forward with a pair of non-traumatic forceps, and a custom-made laryngoscope was used to gain access to the glottis. The nanosuspension (or vehicle for the controls) was instilled into the trachea by means of a syringe and 1.2-mm OD plastic tubing, inserted between the vocal chords. To prevent agglomeration, the nanosuspension was vigorously sonicated before, and repeatedly during, administration.

Behavioral investigation

The rats' spontaneous motor activity was measured, on the Monday of wk 4, 7, or 10 (that is, following the last treatment of the subgroup), using an open field box of 48 × 48 × 40 cm size, equipped with 2 arrays of infrared sensors at floor level and at 12 cm height (Conducta 1.0 System, Experimetria Ltd, Budapest). The animals were placed, after 20–30 min of accommodation in the testing room, individually into the center of the box, and the instrument was recording their horizontal and vertical motor activity in 10-min sessions, based on the interruptions of the infrared beams. From these data, counts, time, and run length of the basic activity forms (ambulation, local activity, rearing, immobility) were computed as follows: More than a 40-mm shift in the location of interrupted beams at the floor level during a time unit of 1 s was interpreted as horizontal activity; less shift, as local activity; and no shift at all, as immobility. Rearing was recorded if beams at floor level and at the higher level were interrupted simultaneously. In earlier works (Vezér et al., 2005, 2007) this method proved sensitive to changes caused by Mn in higher nervous functions.

Electrophysiological investigation

The animals were prepared and used for electrophysiological recording on the four days following the open field test. In urethane anesthesia (1000 mg/kg body weight ip), the animal's head was fixed in a stereotaxic frame, and the left hemisphere was exposed by removing the majority of the parietal bone. The wounds were sprayed with 10% lidocaine, and the exposed dura was protected by a thin layer of petroleum jelly. After 30 min of recovery, silver electrodes were placed on the primary somatosensory (SS), visual (VIS), and auditory (AUD) areas. Electrocorticogram (ECoG) was recorded from these areas for 6 min, and the relative spectral powers of the frequency bands (delta, theta, alpha, beta1, beta2, gamma; standard human electroencephalography [EEG] bands as described in Kandel and Schwartz, 1985) were determined. These were evaluated as such, and were also transformed to an "ECoG index." This is the ratio of band powers, [delta + theta]/[beta1 + beta2], and is a practical descriptor of the cortical activity (Dési and Nagymajtényi, 1999). Then, the same electrodes were used to record sensory evoked potentials (EPs). For somatosensory stimulation, two needles were inserted into the contralateral whiskery skin to deliver square electric pulses (3–4 V, 0.05 ms, 1–10 Hz). Visual stimulation was produced by a high-luminance white light-emitting diode (LED) aimed directly at the rat's right eye, driven by 0.2-ms pulses at 1 Hz. The acoustic stimuli were clicks (1 Hz, 40 dB) guided from a miniature earphone into the animal's right ear via the hollow ear bar. Fifty stimuli of each modality per rat were applied and the evoked activity was recorded. After averaging, latency and duration of the evoked responses were measured manually (for details, see Szabó et al., 2005).

Finally, compound action potential form the rat's tail nerve was recorded. Two stimulating needles (delivering 4- to 5-V, 0.05-ms pulses at 1, 20, and 50 Hz) were inserted into the tail base, and another 2, for recording, 50 mm distally. From the records, the conduction velocity of the nerve was calculated, and from that, refractory period (absolute refractory period was defined as the time span after a nerve discharge within which no second stimulation is possible, while within the subsequent relative refractory period the stimulus sensitivity of the nerve is partially restored; see also Dési and Nagymajtényi, 1999). The change of latency of the somatosensory EP, and change of latency and amplitude of the nerve action potential, with increasing stimulation frequency, and change of latency and amplitude of the nerve action potential, were also investigated as a possible indicator of the action of the treatment on the state of the nervous system (Papp et al., 2004).

All electrophysiological recording and analysis was done by means of the Neurosys 1.11 software (Experimetria Ltd, Budapest, Hungary). During the whole procedure, the principles of the Ethical Committee for the Protection of Animals in Research of the University were strictly followed.

General toxicological investigation

During the treatment period, each rat's body weight was measured each Monday, and once more on the day of sacrifice, and the mean body weight of the groups was plotted against time to see the course of weight gain. Following electrophysiology, the rats were sacrificed by an overdose of urethane, dissected, and the organ weights of the brain, liver, lungs, heart, kidneys, spleen, thymus, and adrenals were measured. From these data, relative weights were calculated by relating organ weights to brain weight. Brain weight was chosen as the calculation basis because it was minimally affected by the treatment (Schärer, 1977).

Electron microscopy and elemental analysis

From 3 rats of each group, brain and lungs were fixed in a 7% formalin bath (isotonic, pH 7.4). The organs were sliced and examined (at the National Institute of Environmental Health, Budapest) using a scanning electron microscope with energy-dispersive x-ray spectroscopy (SEM-EDAX). The microscope was operated in "environmental" mode

(water vapor atmosphere and moderate vacuum, 0.1–20 torr, in the chamber). SEM observations were carried out at various magnifications with 25 kV electron beam energy and ~10 mm working distance. An energy-dispersive x-ray spectrum was collected from the selected areas of the tissue in the 0–10 keV range. The total x-ray count rate was between 1000 and 2000 counts s^{-1}. The elements observed were C, O, Na, Al, P, S, K, Ca, and Mn, with detection limit > 1wt%. The relative elemental composition of the tissue samples was computed directly with the EDAX software.

Evaluation

From the general toxicological, behavioral, and electrophysiological data, group means (±SD) were calculated. The results were tested for significance with one-way analysis of variance (ANOVA), and the post hoc analysis was done by Scheffé's test.

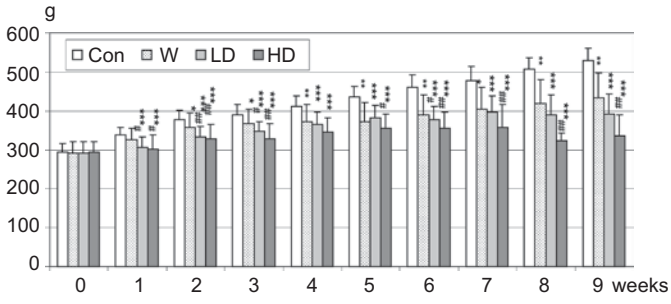

Figure 2. Body weight gain during the 9 wk of intratracheal administration of nanoparticulate Mn. Abscissa, weeks of treatment; ordinate, body weight (mean ± SD). Significance indicated by: *, **, *** $p < .05, .01, .001$ vs. Con; #, ## , ### $p < .05, .01, .001$ vs. W.

Results

General toxicology and tissue manganese detection

Intratracheal instillation had a clear-cut effect on the rats' body weights. There was a normal body weight gain in the control (Con) rats during the treatment period. Compared to that, the vehicle control (W) group had a lower but still uninterrupted weight gain. In both treated groups (HD, LD), however, body weight ceased to increase in wk 6 (Figure 2). Among the relative organ weights (Table 2), weight of the lungs increased strongly with increasing dose and time, and the organs also had, especially in the HD group, a more and more emphysematic exterior (as observed during dissection). It is noteworthy, however, that distilled water instillation (group W) alone had no effect on the lung weight. By wk 9, significant decrease of the liver relative weight developed also. The dose- and time-dependently increased weight of the adrenals was probably secondary, due to stress.

EDAX analysis results indicated that instillation gave rise to substantial internal Mn exposure, which was also in line with the organ weight data. In control rats, no Mn was detected in the lung and brain slices. In rats receiving the highest overall dose, Mn was detected both in lung and the brain samples (Figure 3).

Table 2. Relative organ weights (related to brain weight) after 3, 6, and 9 wk of exposure to Mn nanoparticles.

Groups	Con	W	LD	HD
Relative organ weights, 3 wk				
Lung	1.596 ± 0.479	1.111 ± 0.259	1.955 ± 0.566$^{\#}$	1.911 ± 0.682$^{\#}$
Liver	6.288 ± 00.805	6.431 ± 0.598	5.737 ± 0.684	6.037 ± 0.539
Kidney	1.314 ± 0.107	1.318 ± 0.114	1.260 ± 0.132	1.254 ± 0.094
Heart	0.596 ± 0.040	0.568 ± 0.021	0.565 ± 0.054	0.534 ± 0.058
Spleen	0.366 ± 0.049	0.365 ± 0.055	0.398 ± 0.047	0.396 ± 0.067
Thymus	0.244 ± 0.039	0.246 ± 0.049	0.222 ± 0.049	0.227 ± 0.051
Adrenals	0.027 ± 0.005	0.026 ± 0.005	0.035 ± 0.005	0.034 ± 0.008
Relative organ weights, 6 wk				
Lung	0.845 ± 0.051	0.928 ± 0.461	1.932 ± 0.335$^{***\#\#\#}$	1.959 ± 0.363$^{***\#\#\#}$
Liver	7.121 ± 0.397	7.489 ± 2.670	6.129 ± 0.610	5.986 ± 0.250
Kidney	1.431 ± 0.138	1.508 ± 0.457	1.287 ± 1.117	1.283 ± 0.161
Heart	0.625 ± 0.065	0.628 ± 0.212	0.574 ± 0.089	0.569 ± 0.040
Spleen	0.386 ± 0.036	0.409 ± 0.198	0.369 ± 0.066	0.404 ± 0.089
Thymus	0.239 ± 0.082	0.193 ± 0.079	0.231 ± 0.067	0.248 ± 0.062
Adrenals	0.029 ± 0.004	0.034 ± 0.020	0.032 ± 0.011	0.036 ± 0.008
Relative organ weights, 9 wk				
Lung	0.797 ± 0.055	0.797 ± 0.093	1.614 ± 0.468$^{***\#\#\#}$	2.047 ± 0.426$^{***\#\#\#}$
Liver	7.528 ± 0.665	6.080 ± 1.104**	5.979 ± 0.803**	5.134 ± 0.546$^{***\#}$
Kidney	1.488 ± 0.073	1.332 ± 0.160	1.309 ± 0.263	1.227 ± 0.087**
Heart	0.626 ± 0.034	0.575 ± 0.032	0.597 ± 0.086	0.619 ± 0.091
Spleen	0.390 ± 0.057	0.371 ± 0.048	0.358 ± 0.094	0.317 ± 0.041
Thymus	0.192 ± 0.049	0.148 ± 0.050	0.235 ± 0.060$^{\#\#}$	0.202 ± 0.044
Adrenals	0.024 ± 0.005	0.029 ± 0.006	0.033 ± 0.011	0.041 ± 0.011$^{**\#}$

Note. Significance indicated by: *, **, *** $p < .05, .01, .001$ vs. Con; #, ## , ### $p < .05, .01, .001$ vs. W. For group codes, see Table 1.

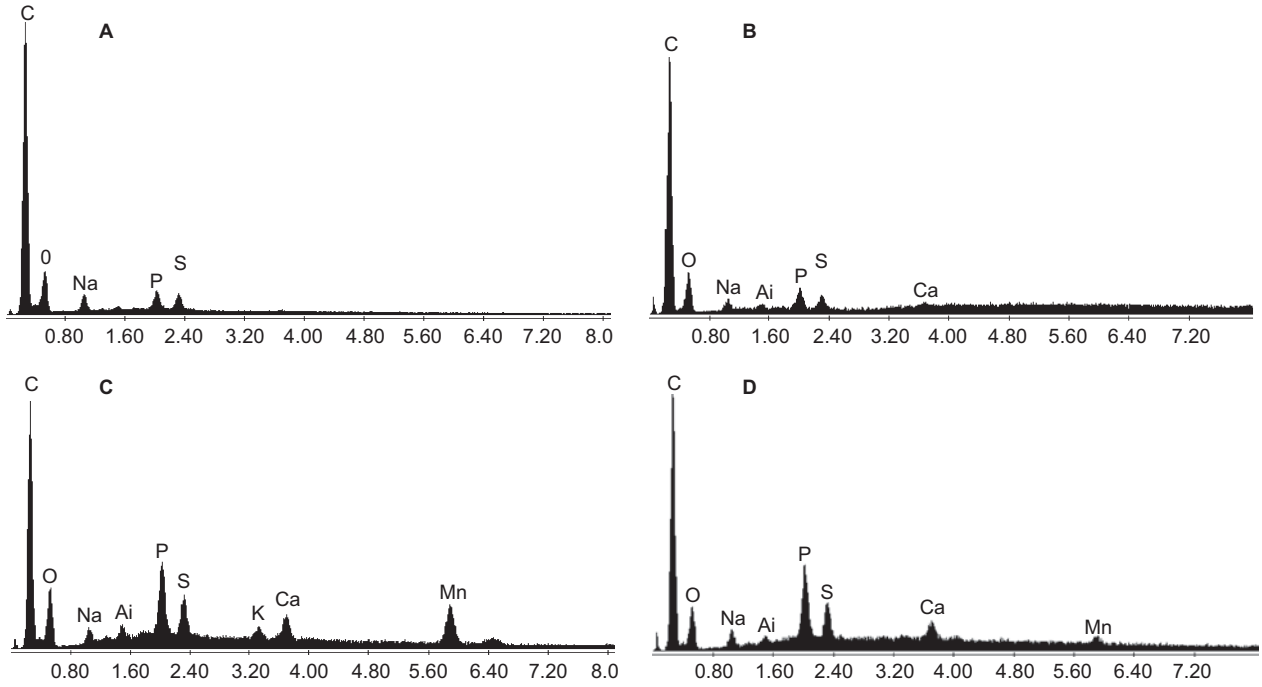

Figure 3. Samples of EDAX analysis spectra of a control lung (A), control, brain (B), and high-dose treated lung (C) and brain (D) tissue. The Mn content (wt%) was zero in the controls, but gave a clear-cut peak in the high dose samples (on the spectra showed, 15.56% and 4.76% in the lung and brain sample, respectively). The ordinate (counts) is the same for all four graphs.

Table 3. ECoG index values from the somatosensory (SS), visual (VIS), and auditory (AUD) cortical area after 3, 6, and 9 wk of exposure to Mn nanoparticles.

		SS	VIS	AUD
3 weeks	Con	1.921 ± 0.418	1.544 ± 0.286	2.229 ± 0.545
	W	2.205 ± 0.363	1.617 ± 0.409	2.388 ± 0.967
	LD	1.974 ± 0.386	1.750 ± 0.437	2.373 ± 0.798
	HD	1.989 ± 0.338	1.513 ± 0.303	2.028 ± 0.577
6 weeks	Con	2.139 ± 0.307	1.584 ± 0.455	2.698 ± 0.924
	W	2.178 ± 0.401	1.879 ± 0.302	2.468 ± 0.676
	LD	1.902 ± 0.299	1.726 ± 0.374	2.269 ± 0.759
	HD	1.722 ± 0.710	1.662 ± 0.460	2.328 ± 1.186
9 weeks	Con	2.335 ± 0.277	1.873 ± 0.209	3.047 ± 0.643
	W	1.983 ± 0.588	1.723 ± 0.468	2.706 ± 1.375
	LD	1.730 ± 0.302*	1.503 ± 0.417	2.364 ± 0.563*
	HD	1.613 ± 0.156***	1.506 ± 0.159*	2.446 ± 0.557

Note. Significance indicated by: *, *** $p < .05, .001$ vs. Con.

Electrophysiological effects

In the spontaneous cortical activity, the treatment caused some increase of the fast, and decrease of the slow, waves, as indicated by the ECoG index data (Table 3). This change was also more prominent with higher dose and longer treatment period.

Among the parameters of evoked activity, lengthening of the latency was the most prominent, developing in a dose- and time-dependent manner to significant changes after 9 wk. In case of the SS EP (Figure 4A), the latency increase was significant in both treated groups versus Con, and also in the HD group versus LD, but only at more frequent stimulation (2 and 10 Hz instead of 1, see insert in Figure 4A). This possibly indicated the increased fatigability of the cortex in the treated rats. The changes in the duration were not as clear-cut (Figure 4B), with the only significant change being a decrease in the HD group at 2 Hz stimulation frequency. In the VIS and AUD EP (Figure 4, C and D, respectively), the most marked effect was also the latency lengthening in the HD group. The negligible difference between the values of the Con and W group showed that the procedure alone (including repeated ether anesthesia) had in itself no influence on the cortical activity.

In the tail nerve, conduction velocity decreased significantly in both treated groups after 9 wk of exposure to Mn NPs (Figure 5A). There was a parallel increase in the absolute refractory period, significant only in the HD group (Figure 5B).

Behavioral effects

The treated rats' open field activity showed a shift to less and less mobility. As seen in Figure 6, there was some decrease of ambulation and increase of local activity and immobility also in the two controls (Con and W), which was mostly due to increasing age of the rats. In the treated groups, especially in HD, the decrease of ambulation and rearing was much more pronounced and had a clear treatment time dependence. The numerical data of OF activity at 9 wk (Table 4) indicate that in the HD group the overall distance and time of ambulation significantly decreased versus both controls and also versus LD, while the time and count of local activity and immobility increased significantly. This, together with the visible but not significant differences between LD and Con or W, shows the same trend of alterations with increasing total dose as was seen in some organ weights and in EP latency.

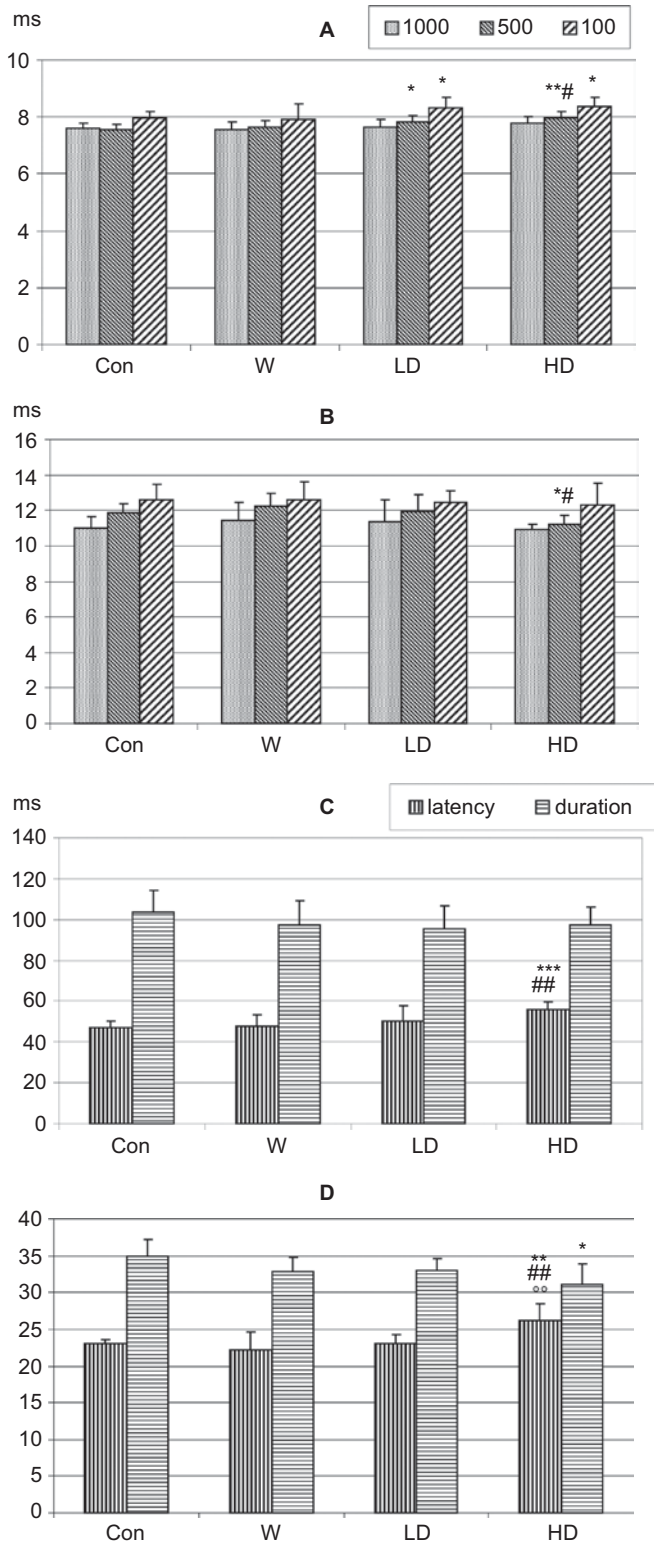

Figure 4. Measured parameters of the cortical evoked potentials after 9 wk of treatment with Mn nanoparticles: (A) latency and (B) duration of the somatosensory evoked potential at various stimulation period times (1000, 500, and 100 ms; see insert in A, corresponding to 1, 2, and 10 Hz stimulation frequency); (C, D) latency and duration of the (C) visual and (D) auditory evoked potentials (see insert in C). Mean + SD, $n=8$. Significance indicated by: *, ** $p<.05$, .01 vs. Con; #, ## $p<.05$, .01 vs. W; °° $p<.01$ vs. LD.

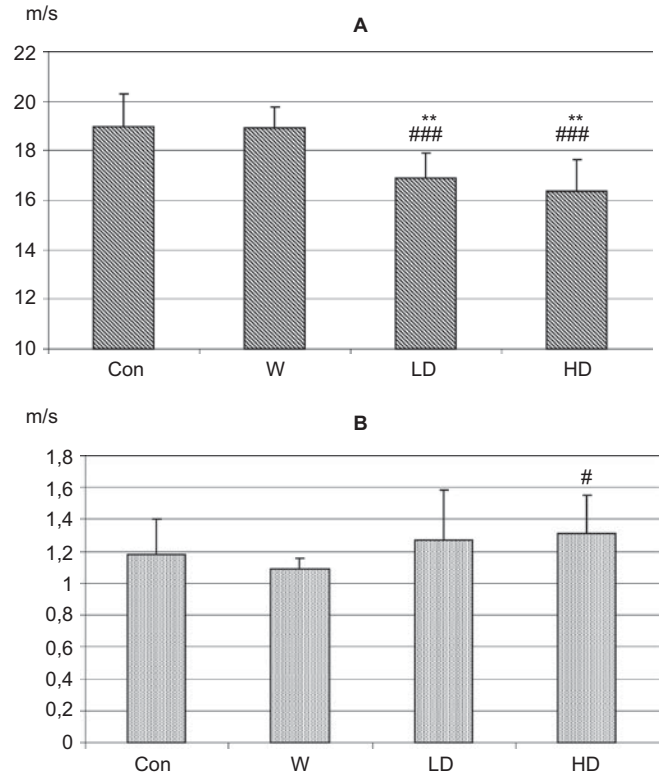

Figure 5. Conduction velocity (A) and absolute refractory period (B) of the tail nerve. Mean + SD, $n=8$. Significance indicated by: ** $p<.01$ vs. Con; #, ### $p<.05$, .001 vs. W.

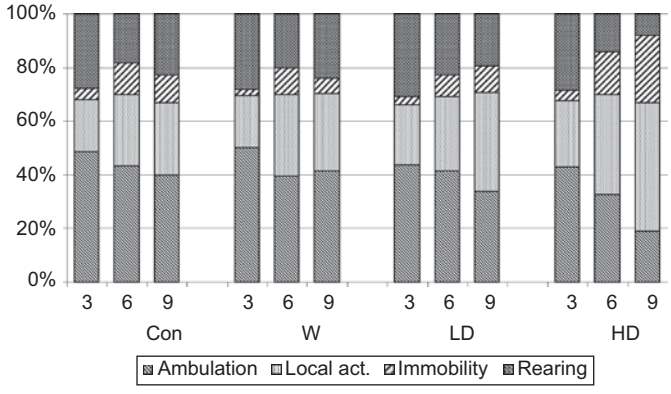

Figure 6. Distribution of the time spent by the rats in the four forms of open field activity (ambulation, local activity, rearing, immobility: see insert below) after 3, 6, and 9 wk of treatment (indicated on the abscissa). Group means, $n=8$. The total height of the bars represents the 10-min length of an OF session.

Discussion

Direct Mn detection and the observed functional alterations both indicate that the Mn content of the instilled nanoparticles had access to the CNS. One possible way of that was migration of the NPs from the site of exposure to the target organs. NPs, in contrast to microscopic particles, appear to translocate readily to extrapulmonary sites and reach other organs by transcytosis across respiratory epithelium into the interstitium, and have access to the blood circulation directly

Table 4. Numerical parameters of the open field activity of the rats after 9 wk of exposure to Mn nanoparticles (mean ± SD, $n = 8$).

	Con	W	LD	HD
Ambulation distance	195.34 ± 45.14	185.05 ± 51.89	155.14 ± 26.17	72.44 ± 40.21**##°
Ambulation time	240.60 ± 55.29	250.20 ± 63.03	204.50 ± 28.18	113.83 ± 50.70**##°
Ambulation count	29.80 ± 6.98	29.00 ± 7.35	29.00 ± 4.20	20.00 ± 5.44
Local activity time	162.20 ± 38.75	171.60 ± 63.03	220.00 ± 61.06	288.00 ± 38.11**#
Local activity count	68.80 ± 15.83	71.60 ± 12.56	81.17 ± 13.23	95.17 ± 5.24*#
Immobility time	61.60 ± 50.16	35.80 ± 19.68	60.17 ± 32.11	150.50 ± 69.36*##°
Immobility count	31.20 ± 16.96	22.60 ± 11.39	32.17 ± 16.77	65.67 ± 16.74*##°
Rearing time	136.60 ± 42.89	143.40 ± 64.89	116.33 ± 81.29	48.67 ± 31.09
Rearing count	51.60 ± 8.23	54.60 ± 18.82	42.67 ± 21.88	25.67 ± 18.34

Note. Significance indicated by: *, ** $p < .05, .01$ vs. Con; #, ## $p < .05, .01$ vs. W; ° $p < .05$ vs. LD.

or via the lymph drainage (Oberdörster et al., 2005). From the blood, Mn NPs enter the brain through the capillary endothelial cells in the blood–brain barrier, and through the choroid plexuses (Crossgrove et al., 2005). A likely alternative is dissolution from the surface of the NPs (Handy et al., 2008). MnO_2 and other stable oxides of Mn are water insoluble but will dissolve in acidic media. Particles in the alveoli are phagocytosed by macrophages and end up in the low pH (~4.5) of phagolysosomes (Lundborg et al., 1985). The released Mn^{2+} ions then can pass the blood–brain barrier (Aschner et al., 1999) and deposit in the brain (Mena et al., 1967). The likely role of dissolution is indicated, e.g., by the similar effect of solute and nanoparticle form of Mn in cell culture (Hussain et al., 2006), and by the similarity of neuro-functional alterations observed in this study and in previous works of us referred to later. Dissolving NPs, beyond being sources of systemic exposure, can generate cytotoxic metal concentrations locally.

Excess Mn is known to cause a multitude of functional abnormalities in humans (Mergler et al., 1999). In case studies on effects of airways exposure by welding fumes, which mainly consist of nanoparticles (McNeilly et al., 2004) and always contain Mn (Antonini et al., 2006), parkinsonism (Bowler et al., 2006) and epileptic syndrome (Hernandez et al., 2003) were mentioned. In the same exposure group, altered EEG and event-related potentials were reported (Sinczuk-Walczak et al., 2001; Sjögren et al., 1996; Wennberg et al., 1991). Previous works of our laboratory revealed cortical electrophysiological changes in rats following acute (Pecze et al., 2005) and subchronic (Vezér et al., 2005) exposure to Mn in the form of orally or intraperitoneally applied $MnCl_2$ solution.

At the cellular level, the most important effects of Mn exposure result from disturbance of energy metabolism. Mitochondrial complex II (Malecki, 2001) and complex III (Zhang et al., 2003) were found to be inhibited by the presence of Mn, leading to insufficiency in energy-demanding processes of neurons like ion pumps (to regain normal resting potential), or to disturbed synthesis, release, reuptake, and postsynaptic reaction to glutamate (Centonze et al., 2001), dopamine (Shinotoh et al., 1997; Yamada et al., 1986), and other transmitters. Tyrosine hydroxylation, a crucial step of dopamine synthesis, was blocked by Mn in vitro (Hirata et al., 2001), possibly by a mechanism depending on inhibition of mitochondrial function.

In rodents exposed experimentally to Mn, morphological changes resembling those seen in Parkinson's disease patients were found (Ponzoni et al., 2000), which underpins the relevance of our animal model, and indicates the involvement of dopaminergic structures in the observed functional alterations. Motivation, and hence open field locomotor activity, are regulated by mesolimbic/mesocortical dopaminergic structures (Alexander et al., 1990). In chronic manganese exposure, liver damage (indicated in our work by the decreased organ weight, see Table 2) can affect the substrate supply for the synthesis of the monoamine neurotransmitters (Verity, 1999). Beyond that, hyperammonemia due to the liver damage may have lead to ammonia-dependent elevation of extracellular glutamate (and further to NMDA-mediated neurotoxicity: Butterworth, 1998).

Mn-dependent inhibition of astrocytic glutamine synthetase (Aschner et al., 1999) also may have contributed to the elevated extracellular glutamate level, another possible consequence of which is enhanced synaptic transmission in the cortex (Hazell and Norenberg, 1997). This may result acutely in increased EP amplitudes, as reported by Pecze et al. (2005) (and also may explain the epileptogenic effect described by Hernandez et al., 2003) and subchronically in increased EP latency as reported by Vezér et al. (2005). In the present work, significant latency lengthening of the EPs was observed, primarily in the rats receiving the highest overall dose.

In the same rats, also the change of the ECoG band activity reached significance. The decrease of slow (delta, theta) and increase of fast (beta1, beta2, gamma) bands was similar to results obtained with another mitochondrial toxin, 3-nitropropionic acid, in subacute exposure (Szabó et al., 2005) and may have resulted from increased collateral input of the (glutamatergic) specific afferents to the ascending reticular activation. As, however, Mn exerts inhibition on choline acetyltransferase (Lai et al., 1981), increased reticular activation may not be the only explanation of faster cortical spontaneous activity in the treated rats.

Pulmonary insufficiency and tissue hypoxia did, most probably, develop in the treated rats, as suggested by the severe state of the lungs observed on dissection (discussed later). This, however, is not a likely explanation of the ECoG changes, as experimental hypoxia in humans (van der Post et al., 2002) and mitochondrial dysfunction (Smith and Harding, 1993) typically cause slowed EEG.

Oxidative stress most probably contributed to the alterations observed on the dissected organs. Pro-inflammatory effect of (Mn-containing) welding fumes follows from induction of oxidative stress (McNeilly et al., 2004). Chronic airways inflammation and fibrosis most likely caused the emphysema seen on the removed lungs. It has been also reported that nanoparticles can get through barriers within the organism that are impermeable for particles in the microscopic range. Similarly to what was observed in our high-dose animals, accumulation of Mn in the brain was observed in rats exposed to welding fumes for 2 mo (Erikson et al., 2004), together with biochemical indicators of oxidative stress. Hyperactivity of the Mn-dependent superoxide dismutase may be one factor leading to oxidative stress due to overproduction of hydrogen peroxide (Weisiger and Fridovich 1973).

Inhalational exposure to Mn will remain, most probably, a current problem of occupational and environmental hygiene, as will the presence and action of nanoparticles. By means of studies like that presented here, the health consequences can be better understood.

***Declaration of interest*:** This work was supported by the Regional University Knowledge Centre for Environmental and Nanotechnology, Szeged, Hungary.

References

Alexander G.E., Crutcher M.D., DeLong M.R., 1990. Basal ganglia-thalamocortical circuits: Parallel substrates for motor, oculomotor, "prefrontal" and "limbic" functions. Prog. Brain Res. 85, 119–146.

Antonini, J.M., Santamaria, A.B., Jenkins, N.T., Albini, E., Lucchini, R., 2006. Fate of manganese associated with the inhalation of welding fumes: potential neurological effects. NeuroToxicol. 27, 304–310.

Aschner, M., Vrana, K.E., Zheng, W., 1999. Manganese uptake and distribution in the central nervous system (CNS). NeuroToxicology 20, 173–180.

Bader, M., Dietz, M.C., Ihrig, A., Triebig, G., 1999. Biomonitoring of manganese in blood, urine and axillary hair following low-dose exposure during the manufacture of dry cell batteries. Int. Arch. Occup. Environ. Health. 72, 521–527.

Bowler, R. Koller, W., Schultz, P.E., 2006. Parkinsonism due to manganism in a welder: Neurological and neuropsychological sequelae. NeuroToxicology 27, 327–332.

Butterworth, R.F. 1998. Pathogenesis of acute hepatic encephalopathy. Digest. 59, 6–21.

Centonze, D., Gubellini, P., Bernardi, G., Calabresi P., 2001. Impaired excitatory transmission in the striatum of rats chronically intoxicated with manganese. Exp. Neurol. 172, 469–476.

Crossgrove, J.S., Yokel, R.A., 2005. Manganese distribution across the blood-brain barrier IV. Evidence for brain influx through store-operated calcium channels. NeuroToxicology 26, 297–307.

Dési I, Nagymajtényi L., 1999. Electrophysiological biomarkers of an organophosphorous pesticide, dichlorvos. Toxicol. Lett. 107, 55–64.

Elder, A., Gelein, R., Silva, V., Feikert, T., Opanashuk, L., Carter, J., Potter, R., Maynard, A., Ito, Y., Finkelstein, J., Oberdörster, G., 2006. Translocation of ultrafine manganese oxide particles to the central nervous system. Environ. Health Perspect. 114, 1172–1178.

Erikson, K.M., Aschner, M., 2003. Manganese neurotoxicity and glutamate-GABA interaction. Neurochem. Int. 43, 475–480.

Erikson, K.M., Dorman, D.C., Lash, L.H., Dobson, A.W., Aschner, M., 2004. Airborne manganese exposure differentially affects end points of oxidative stress in an age- and sex-dependent manner. Biol. Trace Elem. Res. 100, 49–62.

Fechter, L.D., Johnson, D.L., Lynch, R.A. 2002. The relationship of particle size to olfactory nerve uptake of a non-soluble form of manganese into brain. NeuroToxicology 23, 177–183.

Ferraz, H.B., Bertolucci, P.H., Pereira, J.S., Lima, J.G., Andrade, L.A., 1988. Chronic exposure to the fungicide maneb may produce symptoms and signs of CNS manganese intoxication. Neurology 38, 550–553.

Hernandez, E.H., Discalzi, G., Dassi, P., Jarre, L., Pira, E., 2003. Manganese intoxication: The cause of an inexplicable epileptic syndrome in a 3 year old child. NeuroToxicology 24, 633–639.

Handy, R.D., von der Kammer, F., Lead, J.R., Hassellö,v, M., Owen, R., Crane, M., 2008. The ecotoxicology and chemistry of manufactured nanoparticles. Ecotoxicology 17, 287–314.

Hirata, Y., Kiuchi, K., Nagatsu, T., 2001. Manganese mimics the action of 1-methyl-4-phenylpyridinium ion, a dopaminergic neurotoxin, in rat striatal tissue slices. Neurosci. Lett. 311, 53–56.

Hussain, S.M., Javorina, A.K., Schrand, A.M., Duhart, H.M., Ali, S.F., Schlager, J.J., 2006. The interaction of manganese nanoparticles with PC-12 cells induces dopamine depletion. Toxicol. Sci. 92, 4456–463.

Kandel, E.R., Schwartz, J. H., 1985. Principles of Neural Science, Elsevier, New York, pp. 643–644.

Kenangil, G., Ertan, S., Sayilir, I., Ozekmekci, S., 2006. Progressive motor syndrome in a welder with pallidal T1 hyperintensity on MRI: A two-year follow-up. Movement Disorders 21, 2197–2200.

Lai, J.C., Leung, T.K., Lim, L., 1981. Brain regional distribution of glutamic acid decarboxylase, choline acetyltransferase, and acetylcholinesterase in the rat: effects of chronic manganese chloride administration after two years. J. Neurochem. 36, 1443–1448.

Lundborg, M., Eklund, A., Lind, D.B., Camner, P., 1985. Dissolution of metals by human and rabbit alveolar macrophages. Br. J. Ind. Med. 42, 642–645.

Malecki, E.A., 2001. Manganese toxicity is associated with mitochondrial dysfunction and DNA fragmentation in rat primary striatal neurons. Brain Res. Bull. 55, 225–228.

McNeilly, J.D., Heal, M.R., Beverland, I.J., Howe, A., Gibson, M.D., Hibbs, L.R., MacNee, W., 2004. Soluble transition metals cause the pro-inflammatory effects of weiding fumes ion vitro. Toxicol. Appl . Pharmacol. 196, 95–107.

Mena, I., Marin, O., Fuenzalida, S., Cotzias, G.C., 1967. Chronic manganese poisoning: clinical picture and manganese turnover. Neurology 17, 128–136.

Mergler, D., Baldwin, M., Belanger, S., Larribe, F., Beuter, A., Bowler, R., Panisset, M., Edwards, R., de Geoffroy A., Sassine, M.-P., Hudnell, K.,, 1999. Manganese neurotoxicity, a continuum of dysfunction: Results from a community based study. NeuroToxicology 20, 327–342.

Normandin, L., Beaupré, L.A., Salehi, F., St.-Pierre, A., Kennedy, G., Mergler, D., Butterworth, R.F., Philippe, S., Zayed, J., 2004. Manganese distribution in the brain and neurobehavioral changes following inhalation exposure of rats to three chemical forms of manganese. NeuroToxicology 25, 433–441.

Normandin, L., Hazell, A.S., 2001. Manganese neurotoxicity: an update of pathophysiologic mechanisms. Metab. Brain Dis. 17, 375–387.

Oberdörster, G., Oberdörster, E., Oberdörster, J., 2005. Nanotoxicology: An emerging discipline evolving from studies of ultrafine particles. Environ. Health Perspect. 7, 823–839.

Oka, Y., Mitsui, M., Kitahashi, T., Sakamoto, A., Kusuoka, O., Tsunoda, T., Mori, T., Tsutsumi, M., 2006. A reliable method for intratracheal instillation of materials to the entire lung in rats. J. Toxicol. Pathol. 19, 107–109.

Ono, K., Komai, K., Yamada, M., 2002. Myoclonic involuntary movement associated with chronic manganese poisoning. J. Neurol. Sci. 199, 93–96.

Papp, A., Pecze, L, Vezér, T., 2004. Dynamics of central and peripheral evoked electrical activity in the nervous system of rats exposed to xenobiotics. Centr. Eur. J. Occup. Environ. Med. 10, 52–59.

Pecze, L., Papp, A., Nagymajtényi, L., Dési, I., 2005. Effect of acute administration of certain heavy metals and their combinations on the spontaneous and evoked cortical activity in rats. Environ. Toxicol. Pharmacol. 19, 775–784.

Ponzoni, S., Guimaraes, F.S., Del Bel E.A., Garcia-Cairasco, N., 2000. Behavioral effects of intra-nigral microinjections of manganese chloride: Interaction with nitric oxide. Prog. Neuro-Psychopharmacol. Biol. Psych. 24, 307–325.

Roels, H., Meiers, G., Delos, M., Ortega, I., Lauwerys, R., Buchet, J.P., Lison, D., 1997. Influence of the route of administration and the chemical form (MnCl2, MnO2) on the adsorption and cerebral distribution of manganese in rats. Arch. Toxicol. 71, 223–230.

Schärer, K. 1977. The effect of chronic underfeeding on organ weights of rats. Toxicology 7, 45–56.

Shinotoh, H., Snow, B.J., Chu, N.S., Huang, C.C., Lu, C.S., Lee, C., Takahashi, H., Calne, D.B., 1997. Presynaptic and postsynaptic striatal dopaminergic

function in patients with manganese intoxication: A positron emission tomography study. Neurology 48, 1053–1056.

Sinczuk-Walczak, H., Jakubowski, M., Matczak, W., 2001. Neurological and neurophysiological examinations of workers occupationally exposed to manganese. Int. J. Occup. Med. Environ. Health 14, 329–337.

Sjögren, B., Iregren, A., Frech, W., Hagman, M., Johansson, L., Tesarz, M., Wennberg, A., 1996. Effects of the nervous system among welders exposed to aluminium and manganese. Occup. Environ. Med. 53, 32–40.

Smith, S.J., Harding, A.E., 1993. EEG and evoked potential findings in mitochondrial myopathies. J. Neurol. 240, 367–372.

Szabó, A., Papp, A., Nagymajtényi, L., 2005. Effects of 3-nitropropionic acid in rats: General toxicity and functional neurotoxicity. Arh. Hig. Rada. Toksikol. 56, 297–302.

Van der Post J., Noordzij, L.A., de Kam, M.L., Blauw, G.J., Cohen, A.F., van Gerven, J.M., 2002. Evaluation of tests of central nervous system performance after hypoxemia for a model for cognitive impairment. J. Psychopharmacol. 16, 337–343.

Verity, M.A. 1999. Manganese neurotoxicity: A mechanistic hypothesis. NeuroToxicology 20, 489–497.

Vezér, T., Kurunczi, Á,., Ná,ray, M., Papp, A., Nagymajtényi, L., 2007. Behavioral effects of subchronic inorganic manganese exposure in rats. Am. J. Ind. Med. 50, 841–852.

Vezér, T., Papp, A., Hoyk, Z., Varga, C., Náray, M., Nagymajtényi, L., 2005. Behavioral and neurotoxicological effects of subchronic manganese exposure in rats. Environ. Toxicol. Pharmacol. 19, 797–810.

Weisiger, R.A., Fridovich, I., 1973. Superoxide dismutase. Organelle specificity. J. Biol. Chem. 248, 3582–3592.

Wennberg, A., Iregren, A., Struwe, G., Cizinsky, G., Hagman, M., Johansson, L., 1991. Manganese exposure in steel smelters a health hazard to the nervous system. Scand. J. Work. Environ. Health. 17, 255–262.

Yamada, M., Ohno, S., Okayasu, I., Okeda, R., Hatakeyama, S., Watanabene, H., Ushio, K., Tsukagoshi, H., 1986. Chronic manganese poisoning: A neuropathological study with determination of manganese distribution. Acta Neuropathol. 70, 273–278.

Zhang, J., Fitsanakis, V. A., Gu, G., Jing, D., Ao, M., Amarnath, V., Montine, T.J., 2003. Manganese ethylene-bis-dithiocarbamate and selective dopaminergic neurodegeneration in rat: a link through mitochondrial dysfunction. J. Neurochem. 84, 336–346.